

Transient hygrothermal behaviour of a hemp concrete building envelope

A.D. Tran Le^{a,*}, C. Maalouf^{a,*}, T.H. Mai^a, E. Wurtz^b, F. Collet^c

^a GRESPI/Thermomécanique, Université de Reims, Moulin de la Housse BP. 1039, 51687 Reims, France

^b INES-LOCIE, Savoie Technolac, Université de Savoie, Le Bourget du Lac, 73375 Savoie, France

^c Laboratoire de Génie civil et Génie Mécanique, équipe Matériaux-Thermo-Rhéologie, Université Européenne de Bretagne, Rennes 1, France

ARTICLE INFO

Article history:

Received 8 January 2010

Accepted 15 May 2010

Keywords:

Hemp concrete
Whole building HAM simulation
Ventilation strategies
SPARK
Moisture buffering
Energy

ABSTRACT

The sustainable world's economic growth and people's life improvement greatly depend on the use of alternative products in the architecture and construction, such as industrial wastes conventionally called green materials. For this purpose, hemp concrete is more and more recommended by the eco-builders because hemp is a renewable plant, recyclable and does not degrade within time. It corresponds perfectly to the requirements of high environmental quality buildings. The objective of this article is to study transient hygrothermal behaviour of hemp concrete at whole building level. The physical model is one-dimensional and was implemented into the object-oriented simulation environment SPARK, using the finite difference technique with an implicit scheme. The numerical result showed that the use of hemp concrete wall in buildings can ensure good indoor air quality and energy savings in winter. Besides, the combined effect of moisture buffering with the adequate ventilation strategies increases hemp concrete building performance. Our results also suggest that taking into account the hygrothermal transfer at whole building level with heat and moisture production sources has significant effects on predictions.

© 2010 Elsevier B.V. All rights reserved.

1. Introduction

The combined effect of ventilation and moisture buffering of materials to keep the indoor relative humidity (RH) at a very stable level is very important because relative humidity is one of the most important parameter influencing perceived indoor air quality and human comfort [1,2]. High moisture levels can damage construction and inhabitant's health [3,4]. High humidity harms materials, especially in case of condensation and it helps moulds development increasing allergic risks. Consequently, the means keeping the indoor RH is necessary and essential to improve building performance in the terms of indoor air quality (IAQ), energy performance and durability of building envelope.

Indoor moisture levels are result of the amount of vapour water added to the house compared with the amount removed. Several ways in which water vapour is added include moisture sources (human and animal presence, activity and equipment), the moisture release by hygroscopic material surfaces, moisture flows through building envelope, leaks, humidifiers. Ways by which water vapour is removed include air leaks to outdoors and the moisture adsorption by hygroscopic surfaces, etc. A high performance of indoor air quality and low-energy ventilation system must com-

bine two opposite demands: on one side adequate airflow rate to guarantee good IAQ and to keep the indoor relative humidity at a target level, on the other side a minimal airflow rate to reduce ventilation heat loss. Consequently, several researchers have studied the effect of ventilation strategies and the moisture buffering capacity of materials on indoor climate and efficiency of buildings. The effect of ventilation strategies and the resulting indoor humidity on the saving of energy demand of buildings were demonstrated in [5–8]. The recent study of Woloszyn et al. [7] confirmed that the use of moisture buffering materials and relative humidity sensitive (RHS) ventilation are good ways for reducing building energy demand in dwelling buildings and improving the indoor air quality in the buildings by reducing the amplitude of daily moisture variations. In their studied case, the use of RHS system could reduce the mean ventilation rate of 30–40% in the cold period and generate 12–17% of energy saving.

Hemp concrete is more and more recommended by the eco-builders of a sustainable development. This vegetable material has low environmental impact. The researches done until this day [9–11] allowed us to determine its physical properties but there is no works on its use in building envelopes. In comparison with other materials in construction, the hemp concrete has a low heat conductivity, which reduces heat diffusion and thus reduces winter heat losses and protects from summer heat waves. It has also a low mass density, which reduces its storage capacity. However, its density remains higher than classical insulation materials. Besides, since hemp concrete is a hygroscopic material, it has the

* Corresponding authors.

E-mail addresses: anh-dung.tran-le@etudiant.univ-reims.fr (A.D. Tran Le), chadi.maalouf@univ-reims.fr (C. Maalouf).

Nomenclature

C_p	specific heat at constant pressure, $\text{J kg}^{-1} \text{K}^{-1}$
C_{p0}	specific heat of dry material at constant pressure, $\text{J kg}^{-1} \text{K}^{-1}$
C_{p1}	specific heat of water at constant pressure, $\text{J kg}^{-1} \text{K}^{-1}$
D_T	mass transport coefficient associated to a temperature gradient, $\text{m}^2 \text{s}^{-1} \text{K}^{-1}$
$D_{T,v}$	vapour transport coefficient associated to a temperature gradient, $\text{m}^2 \text{s}^{-1} \text{K}^{-1}$
D_θ	mass transport coefficient associated to a moisture content gradient, $\text{m}^2 \text{s}^{-1}$
$D_{\theta,v}$	vapour transport coefficient associated to a moisture content gradient, $\text{m}^2 \text{s}^{-1}$
g	gravity acceleration, m s^{-2}
h_r	radiative heat transfer coefficient, $\text{W m}^{-2} \text{K}^{-1}$
h_M	convective mass transfer coefficient, m s^{-1}
h_T	convective heat transfer coefficient, $\text{W m}^{-2} \text{K}^{-1}$
Le	Lewis number
L_v	heat of vapourization, J kg^{-1}
P_v	vapour pressure, Pa
Q_m	air flow rate, kg s^{-1}
R_v	constant of water vapour, $\text{J kg}^{-1} \text{K}^{-1}$
S	surface area, m^2
T	temperature, K
T_m	mean radiant temperature, K
t	time, s
V	volume, m^3
x	abscissa, m
θ	moisture volumetric content, $\text{m}^3 \text{m}^{-3}$
λ	thermal conductivity, $\text{W m}^{-1} \text{K}^{-1}$
ρ_0	mass density of dry material, kg m^{-3}
ρ_i	air density, kg m^{-3}
ρ_l	mass density of water, kg m^{-3}
ρ_v	mass density of vapour water, kg m^{-3}
ψ	capillary pressure, Pa
ϕ	relative humidity, %
σ_0	Stefan–Boltzmann constant, $\text{W m}^{-2} \text{K}^{-4}$
δ	water vapour permeability, $\text{kg m}^{-1} \text{s}^{-1} \text{Pa}^{-1}$
ε	wall emissivity (long wave)
Φ	heat flux, W
Φ_{ray}	radiation heat flux, W
Φ_{Source}	heat source power, W

capacity to store or release moisture to ambient air so it has ability to moderate the daily or seasonal humidity variations of the indoor environment and even the ability to moderate sudden step change of an indoor moisture level. Furthermore, the grey energy of hemp concrete is 90 kWh/m^3 and very small by comparing with 430 kWh/m^3 of normal concrete and 696 kWh/m^3 of standard brick. Regarding all that, hemp concrete can be considered as a good compromise between insulation, energy efficiency, buffering capacity purpose and green material.

The purpose of this paper is to study the transient hygrothermal behaviour of a hemp concrete building envelope. First the details for the modelling of whole building heat–air–moisture (HAM) simulation are shown. The models were elaborated and implemented in the Simulation Problem Analysis and Research Kernel (SPARK), which is adapted to the complex problems [12]. Then the simulation tools were tested with experimental data available from the Annex 41 “Whole Building Heat, Air and Moisture Response” of the International Energy Agency’s (IEA). After being validated, the model was used to analyze the impact of hemp concrete on indoor

air humidity and air-conditioning loads. The sensitivity analysis of simulation parameters (transport coefficients, thermal conductivity and isotherm sorption curve) and the impact of ventilation rate on the building performance were carried out. Finally, the effect of combining hemp concrete moisture buffering capacity with the different ventilation strategies was investigated and compared to another material used in dwelling buildings: cellular concrete. In the next part, the mathematical model for whole building HAM and its numerical solution will be presented.

2. Mathematical models

2.1. Moisture transport in building materials

Moisture has been identified as a major factor affecting durability of building materials. Moisture accumulation within building components can lead to poor thermal performance of the envelope, metal corrosion and structure deterioration. In addition, moisture transport through building envelopes has a significant effect on indoor air humidity and air-conditioning loads. Understanding and predicting the humidity transfers in building envelope is essential to improve performance and durability of buildings.

Mechanisms of moisture transport in a single building material have been extensively studied [13–17]. Most of the models have nearly the same origin: the Philip and De Vries model [18] and the laws of Fourier, Fick and Darcy. The main difference among them is related to particular assumptions used. Based on Mendes et al.’s work, we used a model that takes into account moisture transport under liquid and vapour [19]. Forms of moisture transport depend on the pore structure as well as environmental conditions. The liquid phase is transported by capillarity whereas the vapour phase is due to the gradients of partial vapour pressure. With these considerations, the mass conservation equation becomes:

$$\frac{\partial \theta}{\partial t} = \frac{\partial}{\partial x} \left(D_T \frac{\partial T}{\partial x} \right) + \frac{\partial}{\partial x} \left(D_\theta \frac{\partial \theta}{\partial x} \right) \quad (1)$$

with the following boundary conditions, respectively, for the external ($x=0$) and internal ($x=L$) surfaces of the wall:

$$-\rho_l \left(D_T \frac{\partial T}{\partial x} + D_\theta \frac{\partial \theta}{\partial x} \right) \Big|_{x=0,e} = h_{M,e} (\rho_{v,a,e} - \rho_{v,s,e}) \quad (2)$$

$$-\rho_l \left(D_T \frac{\partial T}{\partial x} + D_\theta \frac{\partial \theta}{\partial x} \right) \Big|_{x=L,i} = h_{M,i} (\rho_{v,s,i} - \rho_{v,a,i}) \quad (3)$$

where the subscripts a and s represent the adjacent air and solid surface of the material, respectively, while the subscripts e and i correspond, respectively, to the external and internal neighbouring environment (a) or solid surface (s).

The phase change occurring within porous materials acts as a heat source or sink, which results in the couple relationship between moisture and heat transfer. One dimension of the energy conservation equation with coupled temperature and moisture for a porous media is considered and the effect of the adsorption or desorption heat is added. This equation is written as:

$$\rho_0 C_{p_m} \frac{\partial T}{\partial t} = \frac{\partial}{\partial x} \left(\lambda \frac{\partial T}{\partial x} \right) + L_v \rho_l \left(\frac{\partial}{\partial x} \left(D_{T,v} \frac{\partial T}{\partial x} \right) + \frac{\partial}{\partial x} \left(D_{\theta,v} \frac{\partial \theta}{\partial x} \right) \right) \quad (4)$$

where C_{p_m} is the average specific heat which takes into account the dry material specific heat and the contribution of the specific heat of liquid phase.

$$C_{p_m} = C_{p_0} + C_{p_1} \frac{\rho_1}{\rho_0} \theta \quad (5)$$

λ is the thermal conductivity depending on moisture content.

Boundary conditions take into account heat and phase change and radiation, as expressed in the right side of Eqs. (6) and (7) for the external and internal surfaces, respectively.

$$-\lambda \frac{\partial T}{\partial x} - L_v \rho_l \left(D_{T,v} \frac{\partial T}{\partial x} + D_{\theta,v} \frac{\partial \theta}{\partial x} \right)_{x=0,e} = h_{T,e} (T_{a,e} - T_{s,e}) + L_v h_{M,e} (\rho_{v,a,e} - \rho_{v,s,e}) + \Phi_{ray,e} \quad (6)$$

$$-\lambda \frac{\partial T}{\partial x} - L_v \rho_l \left(D_{T,v} \frac{\partial T}{\partial x} + D_{\theta,v} \frac{\partial \theta}{\partial x} \right) \Big|_{x=L,i} = h_{T,i} (T_{s,i} - T_{a,i}) + L_v h_{M,i} (\rho_{v,s,i} - \rho_{v,a,i}) + \Phi_{ray,i} \quad (7)$$

In the case lacking a database of moisture transport coefficients, we have to use simplified models in which we neglect the lacked terms. The use of simplified mathematical models has varying effects on accuracy and has been discussed in [17].

2.2. Mathematical model for the interface

In this section, a wall constituted of two materials *A* and *B* is considered. The heat and mass equations within each material are described in Section 2.1. The interface contact is assumed perfect contact. Therefore we neglect moisture and thermal resistances at the interface between the porous materials. It is possible to state that temperature and capillary pressure are continuous [20]:

$$\begin{cases} (T)_A = (T)_B \\ (\psi)_A = (\psi)_B \end{cases} \quad (8)$$

where *T* is the temperature and ψ is the capillary pressure.

According to Kelvin's law,

$$\phi = \exp \frac{\psi g}{R_v T} \quad (9)$$

It can be deduced using Eq. (8) that:

$$\frac{R_v(T)_A}{g} \ln(\phi)_A = \frac{R_v(T)_B}{g} \ln(\phi)_B \quad (10)$$

where R_v is the constant of water vapour, ϕ is the relative humidity and *g* is the gravity acceleration. Since the temperature for both materials are the same at the interface, Eq. (10) turns into:

$$(\phi)_A = (\phi)_B \quad (11)$$

which means that relative humidity is the same at the interface for both materials while moisture content is discontinuous because they have different pore structures.

2.3. Room modelling details

In order to model heat and mass transfer in the room, we used a nodal method, which considers the room as a perfectly mixed zone characterized by a pressure, a temperature and a moisture concentration. Nodal method involves equations for air and moisture mass balance, heat balance for ambiance and equations describing heat and mass transfer through the walls, additional convection between inside wall surfaces and room ambiance and radiation exchange between inside wall surfaces.

Equations describing heat and mass transfer through the walls were presented in the first section of this paper. The energy balance equation for the air zone can be written as:

$$(\rho_i c_p V + I) \frac{\partial T}{\partial t} = \Phi_{West} - \Phi_{East} + \Phi_{South} - \Phi_{North} + \Phi_{Bottom} - \Phi_{Top} + \Phi_{Source} \quad (12)$$

where *I* is the room thermal inertia. This equation involves heat fluxes through the envelope (from walls and openings) and internal heat sources.

The humidity condition in the room is due to moisture transfer from interior surfaces, moisture production rate and the gains or losses due to air infiltration, natural and mechanical ventilation as well as sources or sinks due to habitants of room. This yields to the following mass balance equation for room air:

$$V \frac{\partial \rho_i}{\partial t} = Q_{mWest} - Q_{mEast} + Q_{mSouth} - Q_{mNorth} + Q_{mBottom} - Q_{mTop} + Q_{mSource} \quad (13)$$

Concerning radiation heat exchange between room walls it was computed using the mean radiant temperature method in which the radiative flow between a wall and all the other walls of the room is written as:

$$\Phi_{rad,LW}^{int} = h_r S (T - T_m) \quad (14)$$

The value of h_r is expressed by:

$$h_r = 4\varepsilon\sigma_0 T_m^3 \quad (15)$$

where T_m is the mean radiant temperature of the walls and is given by:

$$T_m = \frac{\sum S_j T_{Sj}}{\sum S_j} \quad (16)$$

The mass convection coefficient can be estimated using Lewis relation:

$$Le = \frac{h_T}{h_M \rho C_p} = 1 \quad (17)$$

3. Numerical resolution and model validation

3.1. Simulation environment SPARK

The previous equation system has been solved using the finite difference technique with an implicit scheme. Details of discretization are shown in [21].

The Simulation Problem Analysis and Research Kernel (SPARK), a simulation environment allowing to solve efficiently differential equation systems [12,22–24], has been used to solve this set of equations. SPARK was developed by the Simulation Research Group at Lawrence Berkeley National Laboratory. Description of a problem for SPARK solution begins by breaking it down in an object-oriented way. This means thinking about the problem in terms of its components. Each component is represented by a SPARK object that contains the mathematical model for the specific component. Since there may be several components of the same kind, SPARK object models, equations or group of equations, are defined in a generic manner called classes. Classes serve as templates for any number of objects required to formulate the whole problem. The problem model is then completed by linking objects together. Using graph theoretic techniques, SPARK reduces the size of the equation system and uses a Newton–Raphson iterative method to solve the reduced system and after convergence, solves for the remaining unknowns.

3.2. Model validation

International Energy Agency (IEA) has published series of test suites for the validation of whole buildings HAM simulation. These experimental results are used to validate our present model. The measurements have been done in Fraunhofer-Institut Fur Bauphysik, Germany, in the framework of Annex 41. The test room has a floor area of 20 m² and a volume of 50 m³. The walls of the rooms were

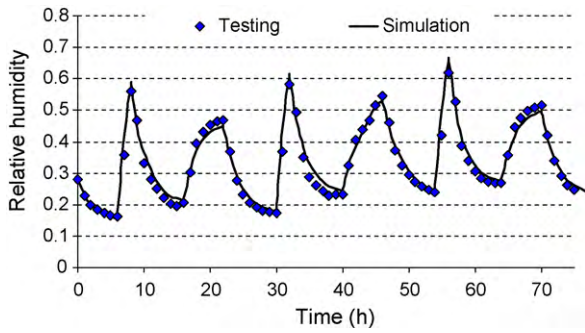


Fig. 1. The validation of simulated results with experimental data.

built with 24 cm of brick and 7 cm polystyrene exterior insulation. Wall and ceiling of the test room was fully coated with aluminium foil and then covered with PVC linoleum. The double-glazed window with dimensions of 1.41 m × 1.94 m is included in the southern wall. The calibrated heating, ventilation and moisture production systems are installed in the rooms. The test is performed with a constant air change rate of 0.5 ach. Detailed descriptions of the experiments and material properties which were measured in laboratory conditions can be found in Annex 41 report [25,26].

Fig. 1 shows the good agreement between the numerical and experimental results. The computed indoor RH is slightly larger than experimental results and the difference is the largest for minimum and maximum values. The same observation is obtained in [27] and that could be explained by the moisture buffering effect of the walls which retards the dynamic equilibrium in the experiment. However, the comparison shows that the model is satisfying to investigate the hygrothermal behaviour of hemp concrete at whole building level. In next section, we will present physical properties of hemp concrete and simulation conditions.

4. Properties of hemp concrete

Hemp is an annual plant which provides two materials used in civil engineering: hemp hurds (granular form of hemp descended from the inner woody core) and hemp fiber (fibrous form of hemp descended from the back-like bast fibers). Hurds are used in lime-hemp render, in hemp mortar and in hemp concrete, while hemp fiber is used in hemp wool. In this article, we are interested in hemp concrete case. Nowadays hemp concrete is widely used in buildings because it is environmentally friendly material suited to the context of sustainable development. The available data of hemp concrete from [9] allow using the transport coefficients as a function of moisture content.

The basic dry material properties are given in Table 1.

The sorption isotherm of hemp concrete which designates the relationship between the moisture content and the relative humidity at a fixed temperature was performed according to the discontinuous method and is shown in Fig. 2. The experimental data are curved fitted with a logarithmic model which balanced relation between functions $\ln(\theta/\theta_s)$ and $\ln(\phi)$ through an exponential correlation proposed in [28]:

$$\ln\left(\frac{\theta}{\theta_s}\right) = a \ln(\phi) \exp(b\phi) \tag{18}$$

Table 1
The dry basic material properties of hemp concrete.

Material	Mass density (kg/m ³)	Thermal conductivity (W/m K)	Specific heat (J/kg K)
Hemp concrete	413	0.1	1000

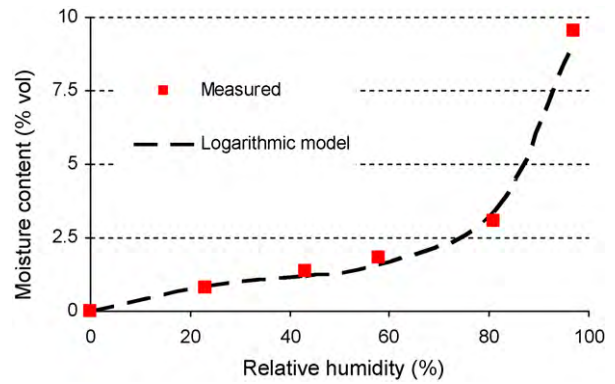


Fig. 2. Sorption isotherms curves for hemp concrete.

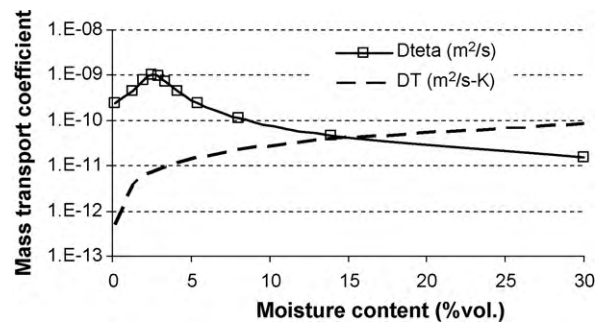


Fig. 3. Mass transport coefficients for hemp concrete.

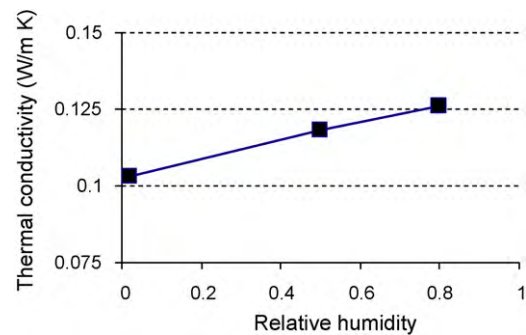


Fig. 4. Thermal conductivity for hemp concrete.

where a designates an intrinsic thermodynamic parameter which depends on the adsorption direction and temperature; b is a parameter employed to improved experimental interpolation. For the hemp concrete case: $a = 1.1$, $b = 2.1$ and $\theta_s = 11.85\%$.

Fig. 3 shows transport coefficients D_T and D_θ for hemp concrete which are responsible for the flow of liquid due to a temperature gradient and a moisture content gradient.

The thermal conductivity is presented in Fig. 4 as a function of relative humidity.

5. Simulation conditions

The plan of the studied room is depicted in Fig. 5. The room has a space area of 15 m² and a volume of 42.75 m³. The ceiling, the west and south facades are in contact with outdoor conditions while other walls are considered as internal partitions and in contact with heated space at 20 °C temperature and 60% relative humidity. External walls and ceiling have 30 cm thickness and partitions 20 cm. It is considered that no moisture diffusion occurs through the floor.

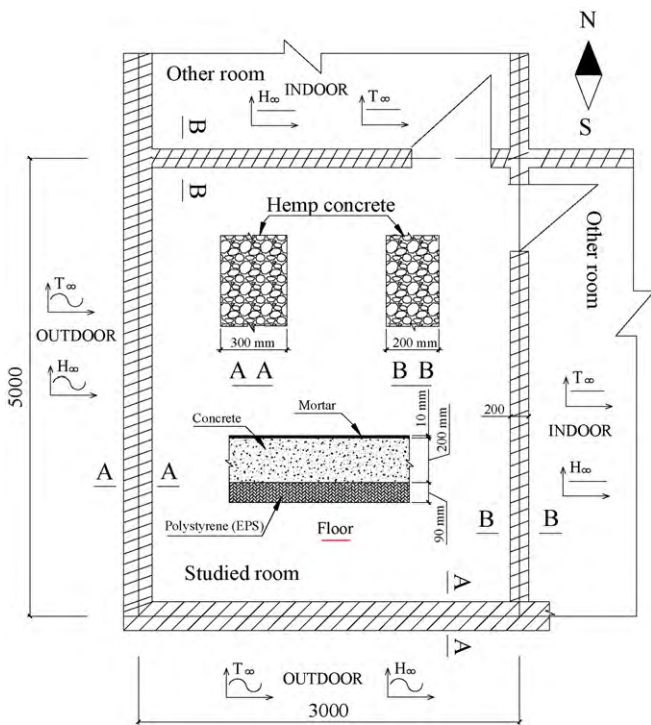


Fig. 5. Plan of studied room.

The room is equipped with a heat sink and a PI controller that keeps indoor temperature around 20 °C. Room is ventilated at 0.5 ach. Heat transfer coefficients are $h_{T,e} = 25 \text{ W/m}^2 \text{ K}$ for the outdoor surfaces and $h_{T,i} = 8 \text{ W/m}^2 \text{ K}$ for indoor surfaces. The mass convection coefficients were calculated using Lewis relation and considering Lewis number equals to 1, which gives for the external and internal surfaces as 0.025 m/s and 0.008 m/s, respectively. Two cases were studied in this article and the details are shown in Table 2. During the occupied period, the interior heat production increases to 160W and moisture production increases to $1.65 \text{ g m}^{-3} \text{ h}^{-1}$. The initial relative humidity and temperature in the walls and the studied room are, respectively, equal to 60% and 20 °C. Simulations are run for the month of January in winter condition of Nancy weather data (in France). The wall is divided into 15 nodes. Time step is 120 s.

Fig. 6 shows the outdoor temperature and outdoor relative humidity for 1 month in January in Nancy. We noted that during the night the outdoor temperature dropped down and the outdoor relative humidity could increase to saturated value of 100%.

6. Results and discussions

This section is dedicated to investigate the effects of the hygrothermal behaviour of hemp concrete walls at whole building level. In Section 6.1 we will present the comparison results between the **Th** and **HAM** models. Sections 6.2, 6.3 and 6.4 show the effects

Table 2
Details of simulations cases and models.

Th	Simulation without taking into account the whole building heat and mass transfer.
HAM	Simulation with taking into account the whole building heat and mass transfer.
Case 0	It considers the test room is unoccupied all time of the day.
Case 1	It considers the test room is occupied during the night time by two persons from 22:00 pm to 8:00 am next day and unoccupied the rest of the day.

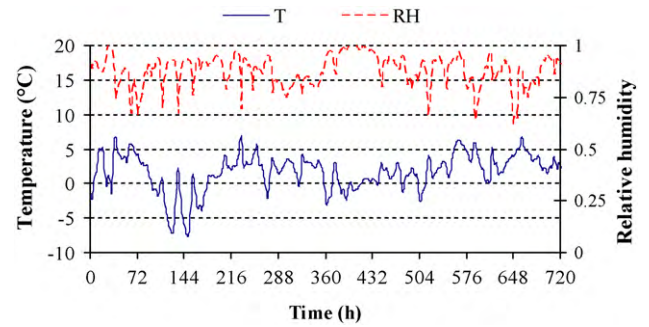


Fig. 6. Outdoor temperature and outdoor relative humidity in January in Nancy.

of simulation parameters, the ventilation rate and external layers on predictions. Section 6.5 presents the comparison between hemp concrete and cellular concrete buildings in terms of building performance. The effect of combining ventilation strategies with moisture buffering materials is investigated in Section 6.6.

6.1. Effect of coupled heat and mass transfer in air-conditioned hemp concrete rooms

In this section, the simulated results of the two models **Th** and **HAM** are investigated. Fig. 7 shows the variation of indoor relative humidity for both models **Th** and **HAM** and for the two cases described in Section 5: with and without taking into account the heat source and moisture production. The results reveal that taking into account the whole building moisture transfer has great effect on indoor relative humidity, and it dampens its variations. For the **HAM** model, moisture buffering capacity of hemp concrete allows it to interact fast with indoor air and thus dampens indoor relative humidity variation. In this case, a difference of 29% for the case 0 and 20% for the case 1 can be noticed between the two models. Besides, in the case 1 the indoor relative humidity is higher due to occupants.

Table 3 summarizes the computed results for the indoor relative humidity and heating energy for the two models and for both cases. In winter, the indoor relative humidity varies between ((32% and 60%) in case 0, (38% and 60%) in case 1) for the **HAM** model compared to one range of ((13% and 60%) in case 0, (16% and 60%) in case 1) for the **Th** model. So we notice that neglecting moisture transfer through building envelope leads to significant errors on the indoor relative humidity profile for both cases (0 and 1). Concerning the heating energy, the computed results show that total energy consumption of the **HAM** model is about 2.2% and 2.4% bigger than in the **Th** model for the cases 1 and 0, respectively, meaning that the

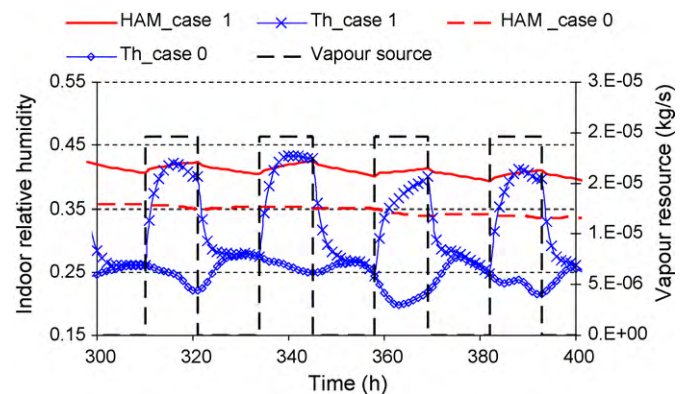


Fig. 7. Variation of indoor relative humidity for the two models and for both cases: with and without taking into account the heat source and vapour production.

Table 3
Average of indoor relative humidity and heating energy for both models and for two cases studied.

	Th_case 1	HAM_case 1	Th_case 0	HAM_case 0
Heating energy (kWh/month)	271.76	277.15	323.11	331.77
Average of indoor RH	0.34	0.42	0.26	0.37
RH (min)	0.16	0.38	0.13	0.32

moisture transfer in building construction does not have a significant effect on heating energy. The similar conclusions can be found in [17,27,29]. This small higher heating energy could be explained by the higher value of thermal conductivity due to higher moisture contents in hemp concrete walls of HAM model. Besides, case 0 could overestimate monthly heating energy up to 19.5%. Therefore, case 1 is used in next sections in which we analyze the sensitivity of indoor relative humidity and energy consumption to simulation parameters such as transport coefficients, thermal conductivity and the sorption curve.

6.2. Sensitivity analysis

6.2.1. Transport coefficients

In this part, we will investigate the impact of measurement accuracy of transport coefficients D_T and D_θ on the prediction of building performance. Fig. 8 shows the impact of mass transport coefficient associated to a temperature gradient on indoor relative humidity. The indoor RH for $1.5 \times D_T$ case is smaller than for $0.5 \times D_T$ case because increasing D_T leads to an increase of the moisture flow through walls from the internal side to the external side (in winter conditions). However, one can observe that even 50% error in D_T value has extremely slight effect on indoor RH predictions. For the energy consumptions, the same conclusion is obtained.

The impacts of mass transport coefficient associated to a moisture gradient on indoor RH and heating energy are shown in Fig. 9. It can be seen that is increasing 25% the coefficient D_θ to $1.25 \times D_\theta$

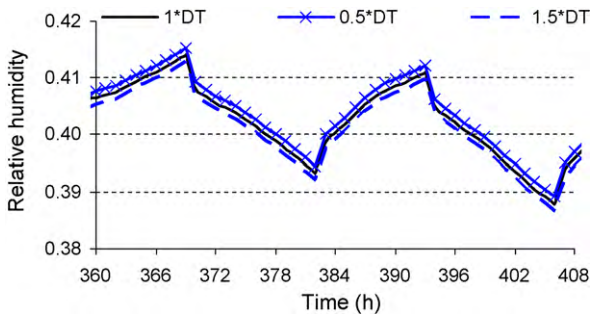


Fig. 8. Impacts of D_T (mass transport coefficient associated to a temperature gradient) on indoor RH.

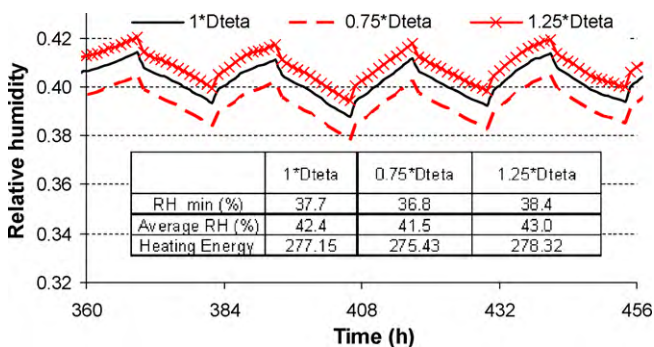


Fig. 9. Impacts of D_θ (mass transport coefficient associated to a moisture gradient) on indoor relative humidity and energy consumption (kWh/month in January).

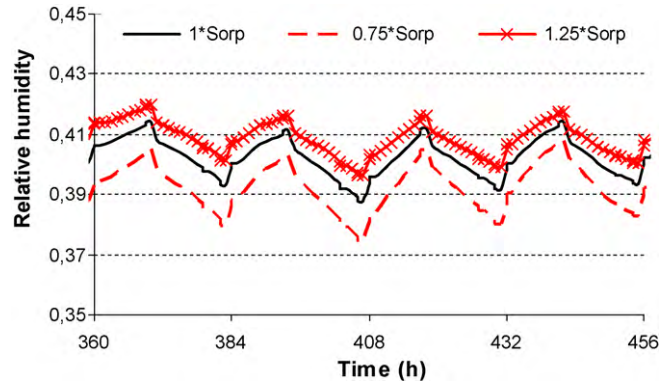


Fig. 10. Impact of sorption isotherm in indoor relative humidity.

case has a slight effect on the RH which is increased about 1.85%. The heating energy increases about 0.42%. We notice in this case that indoor relative humidity increases because of the increase in moisture transfer through partitions.

6.2.2. Thermal conductivity

We compare the results for two cases: one considers the variable thermal conductivity as a function of relative humidity and the second in which the thermal conductivity is assumed constant. The computed results show that the indoor RH in both cases is very close and it is not depicted there. However, the error caused by assuming thermal conductivity to be constant can be larger in terms of energy consumption. The heating energy in January is 262.3 kWh in the constant thermal conductivity case compared to 277.15 kWh in variable thermal conductivity which leads to 5.4% underestimate of energy consumption.

6.2.3. Moisture buffering effect

Fig. 10 shows the impact of the sorption isotherm on the indoor relative humidity. A 25% error in the sorption isotherm value leads to 2.4% error of indoor RH on predictions and to 0.72% error on energy consumption estimation (Table 4). This small effect could be explained by two opposite tendencies concerning energy behaviour of buildings due to moisture buffering materials capacity: On one hand, increasing sorption isotherm leads to more heating energy saving due to the moisture accumulation in hygroscopic materials which will release energy and on the other hand, the higher thermal conductivity due to this process will give more heat loss through the walls.

6.3. Ventilation rates effect

Fig. 11 shows the variation of the average indoor relative humidity as a function of the ventilation rate for the case 1. The results

Table 4
Summarized results of impacts of sorption isotherm on indoor RH and energy consumption.

	1 × Sorp	0.75 × Sorp	1.25 × Sorp
RH_min	0.38	0.36	0.39
Average RH	0.42	0.41	0.43
Heating energy	277.15	275.42	278.16

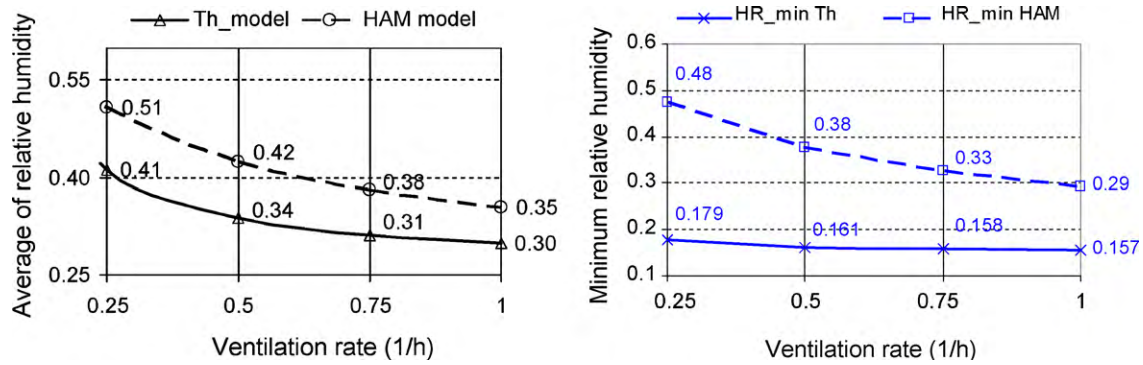


Fig. 11. Average of indoor relative humidity and minimum indoor relative humidity as a function of the ventilation rate for the case 1.

show that as the ventilation rate increases, indoor relative humidity average value decreases and tends to that of the **Th** model. Decreasing the ventilation rate from 1 ach to 0.25 ach, increases the minimum indoor relative humidity from 29% to 48% and thus improved significantly indoor conditions in buildings during the winter. The variation of heating energy as a function of ventilation rate is presented in Fig. 12. Reducing ventilation rate from 1 ach to 0.25 ach decreased heating energy from 385 kWh to 221.7 kWh for **HAM** model and from 366.4 kWh to 224.4 kWh for **Th** model. One can see that heating energy decreases linearly with the ventilation rate. This linear relationship has been approached by two linear functions with an accuracy at least $R^2 = 0.9994$. The linear function slope of **HAM** model is bigger than in the **Th** model (221.93 for **HAM** compared to 189.25 for **Th** model) meaning that the heating energy decreases more quickly with the ventilation rate in the **HAM** model. At low ventilation rate as 0.25 ach, it is surprising to see that energy consumption of **HAM** model becomes lightly smaller than in the **Th** model. This may be explained by the effect of moisture buffering of materials in the **HAM** model which takes into account moisture accumulation in hemp concrete walls which releases heat energy. The higher indoor relative humidity is, the higher moisture accumulation in hemp concrete walls will be. On the other hand, increasing the thermal conductivity due to higher moisture content in walls increases heating energy requirement.

These results show that it is possible to save heating energy in winter season by combining the moisture buffering capacity of materials with ventilation rate strategies [7,30]. Such control strategies are carried out and presented in Section 6.5.

6.4. External mortar layers effects

In this study we investigate the effect of external mortar layers on indoor relative humidity and heating energy (e.g. mortars,

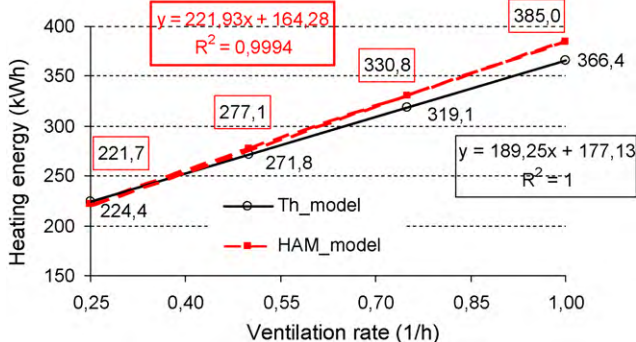


Fig. 12. Heating energy as a function of the ventilation rate for both **Th** and **HAM** models.

hemp mortars, paint, etc.). The walls and ceiling have the same thickness as Fig. 5 and they are made of a triple layer of hemp concrete and two layers of 10 mm of mortar from the inside and outside faces. The material properties of mortar can be found in WUFI [31]. The presence of external layers can decrease the vapour exchanged between the wall and indoor room air so it reduces the moisture buffering effect of hemp concrete. Fig. 13 shows the external mortar layers effects on the variation of indoor relative humidity and energy consumption for 1 month in January.

Computed results indicate that these effects are significant and lead to an overestimation of 4.23% of heating energy use and to an underestimation of 19.1% of the average indoor relative humidity. We notice that the use of external mortar layers decreases the RH average value and the damping effect. The effects are due to the higher conductivity values of mortar and to its lower vapour diffusivity. Our results suggest that external materials with low conductivity and high moisture buffering capacity would suit better to profit the hygroscopic capacity of hemp concrete walls and to increase consumption reductions.

6.5. Comparison between hemp concrete room and cellular concrete room envelopes

Cellular concrete is being used widely due to its lightweight, insulating properties, fire resistance, chemical resistant and structural properties [32]. The purpose of this section is to compare the behaviour of hemp concrete envelope with a cellular concrete one in terms of energy reduction and moisture buffering effect. The material properties of cellular concrete can be found in WUFI [31] and the dry basic material properties are shown in Table 5.

The sorption isotherm of cellular concrete is shown in Fig. 14. The experimental data are curved fitted with a logarithmic model

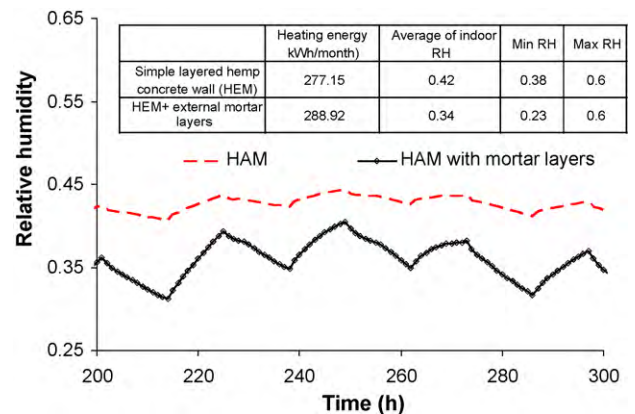


Fig. 13. Variation of indoor relative humidity in the cases with and without external mortar layers and summarized computed results.

Table 5
The dry basic material properties of cellular concrete from WUFI [31].

Material	Mass density (kg/m ³)	Thermal conductivity (W/m K)	Specific heat (J/kg K)
Cellular concrete	600	0.14	850

Table 6
Description of the studied ventilation strategies.

Ventilation strategies	Description
VS.1	Constant ventilation rate (0.5 ach)
VS.2	Sensitive RH ventilation (Fig. 17)
VS.3	Constant ventilation rate and constant indoor RH value

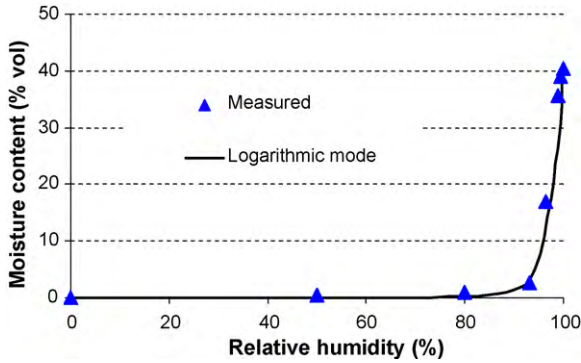


Fig. 14. Sorption isotherms curves for cellular concrete WUFI [31].

conditions for the hemp concrete room and cellular concrete room are presented in Fig. 16. We notice that indoor relative humidity for the hemp concrete room is more dampened. While the minimum indoor RH for the hemp concrete room is 38%, its value decreases to 22% in the cellular concrete case. The indoor RH average value is 42% for the hemp concrete case and 35% for the cellular concrete case. This difference is due to the effect of material hygroscopic capacity. At the same RH, hemp concrete moisture content is higher than that of cellular concrete and thus it can regular better indoor RH.

Concerning the energy consumption, we notice that the use of hemp concrete leads to a reduction of 45% than the case using cellular concrete. This is due to lower thermal conductivity of hemp concrete.

6.6. Effect of ventilation strategies

The results presented above show that the effect of ventilation rates and moisture buffering capacity of hemp concrete have a significant effect on building hygrothermal performance. On one hand, moisture sorption in hemp concrete walls during the occupied period releases energy which decreases heating energy input. On another hand, more heating energy is needed to dry moisture from walls during unoccupied period. Therefore, it may be possible to improve building performance by combining hygroscopic material capacity with adequate ventilation use which guarantees good indoor air quality. Woloszyn et al. [7] confirmed that sensitive relative humidity ventilation is a good way for reducing energy demand in residential buildings. In this section, simulations were performed with three ventilation strategies which are shown in Table 6.

Fig. 17 shows the studied ventilation strategy for the VS.2 in which the ventilation rate varies from 0.2 ach to 0.5 ach when the indoor RH varies from 40% to 60%.

The indoor relative humidity variations for three ventilation strategies are compared and the results for the 16th–17th days are shown in Fig. 18. For the VS.3 strategy, indoor RH is kept constant at 50% through the use of a moisture source. The simulated results in Table 7 show that the minimum values of indoor RH are approximately 45% for VS.2 and 38% in the case of constant ventilation rate (VS.1).

Table 7 shows that the heating energy consumption in VS.2 case (with variable ventilation rate) is about 14.6% and 24.2% lower than in the VS.1 (constant ventilation rate) and VS.3 (constant ventilation rate and indoor RH control) cases, respectively, because the

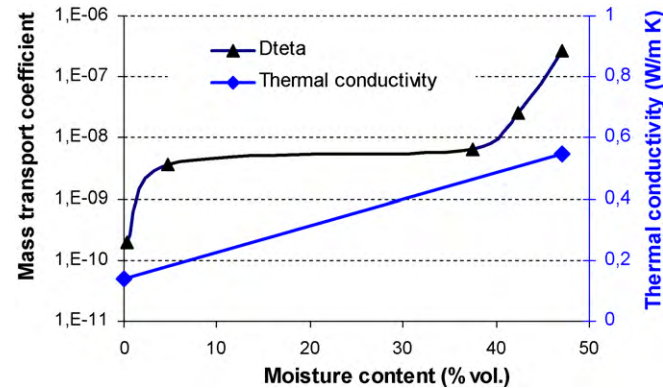


Fig. 15. Transport coefficient D_θ and thermal conductivity of cellular concrete WUFI [31].

[28] in which the coefficients a and b are equal to 2 and 3.1, respectively.

Fig. 15 shows transport coefficient D_θ and thermal conductivity for cellular concrete as a function of moisture content.

First, regarding the grey energy which takes into account the amount of energy required to the product extraction, its manufacture, package and transport. For hemp concrete it is 90 kWh/m³ while it is 400 kWh/m³ for cellular concrete. Concerning the hygrothermal behaviour, the variation of indoor relative humidity and heating energy for 1 month in January for Nancy's winter

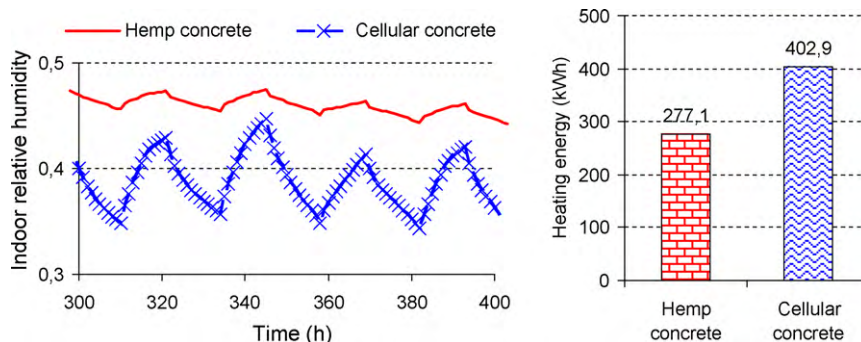


Fig. 16. Variation of indoor relative humidity and heating energy for hemp concrete room and for cellular concrete room.

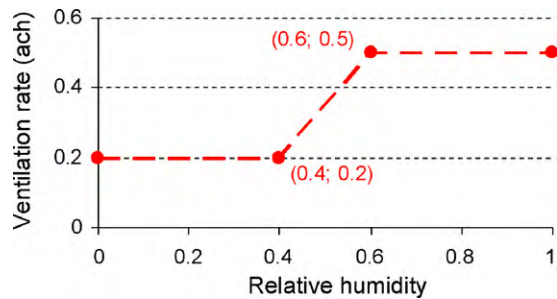


Fig. 17. Relative humidity sensitive ventilation system for the VS.2.

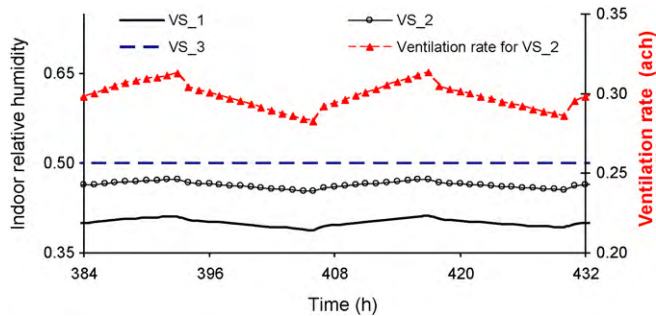


Fig. 18. Indoor relative humidity variation for the three studied ventilation strategies.

Table 7

Summarized results for the three ventilation strategies.

Ventilation strategies	Min_RH	Max_RH	Average of RH	Energy consumption (kWh/month)
VS.1	0.38	0.60	0.42	277.1
VS.2	0.45	0.60	0.48	236.7
VS.3	0.497	0.60	0.50	293.71

average value of ventilation rate in this case is 0.3 ach which is 40% smaller compared to the other cases (0.5 ach). Therefore, the average value of cold fresh air flowing into the room will decrease and results in significant improvement in heating energy reduction in the winter. The results also reveal that energy consumption for VS.3 is the highest.

7. Conclusions

In this article, we used a couple heat and mass transfer model at whole building level to analyze the transient hygrothermal behaviour of a hemp concrete building envelope. The model was implemented in SPARK, an object-oriented program suited to complex problems.

In order to validate the simulation tools, simulations were run and the numerical results were compared to experimental data available from Annex 41 in the frameworks of the International Energy Agency. A good agreement between experimental and numerical results was found. The model was then applied to investigate the transient hygrothermal behaviour of hemp concrete in buildings. Our results show that taking into account moisture transfer and indoor heat and moisture production sources has a significant effect on indoor relative humidity and energy consumption predictions. Differences of about 65% in indoor relative humidity and 19.5% in energy consumption were found. Simulations were used to investigate hemp concrete moisture buffering capacity where it was shown that hemp concrete can decrease the daily indoor relative humidity variations. A sensitivity analysis was also carried out and it showed that envelope hygrothermal per-

formance is very sensitive to ventilation rate and to the physical properties of wall coating or external layer. Besides, hemp concrete behaviour was compared to that of cellular concrete and it was found that reduction of 45% in energy consumption can be reached with hemp concrete. Finally different ventilation strategies were compared and it was found that the use of a sensitive relative humidity ventilation strategy with hemp concrete can reduce energy consumption about 15%.

References

- [1] L. Fang, G. Clausen, P.O. Fanger, Impact of temperature and humidity on perception of indoor air quality, *Indoor Air* 8 (1998) 80–90.
- [2] L. Fang, P. Wargocki, T. Witterseh, G. Clausen, P.O. Fanger, Field study on the impact of temperature, humidity and ventilation on perceived air quality, in: *Proceeding of the 8th International Congress on Indoor Air Quality*, vol. 2, Edinburgh, UK, 1999, pp. 107–112.
- [3] C.G. Bornehag, G. Blomquist, F. Gyntelberg, B. Jarvholm, P. Malmberg, L. Nordvall, et al., Dampness in buildings and health. Nordic interdisciplinary review of the scientific evidence on associations between exposure to “dampness” in buildings and health effects (NORDDAMP), *Indoor Air* 11 (2) (2001) 72–86.
- [4] C.G. Bornehag, J. Sundell, S. Bonini, A. Custovic, P. Malmberg, S. Skerfving, et al., Dampness in buildings as a risk factor for health effects. EUROEXPO: a multidisciplinary review of the literature (1998–2000) on dampness and mitre exposure in buildings and health effects, *Indoor Air* 14 (4) (2004) 243–257.
- [5] J. Jokisalu, J. Kurnitski, *Simulation of Energy Consumption in Typical Finnish Detached House*, Helsinki University of Technology, HVAC Laboratory, report B74, 2002.
- [6] A. Afshari, N.C. Bergsøe, Humidity as a control parameter for ventilation, *Indoor and Built Environment* 12 (2003) 215–216.
- [7] M. Woloszyn, T. Kalamees, M.O. Abadie, M. Steeman, A.S. Kalagasidis, The effect of combining a relative-humidity-sensitive ventilation system with the moisture-buffering capacity of materials on indoor climate and energy efficiency of buildings, *Building and Environment* 44 (2009) 515–524.
- [8] K. Juslin, *Analyse multicritères des stratégies de ventilation en maisons individuelles*, Thèse de doctorant, Université de La Rochelle, 2009.
- [9] F. Collet, *Caractérisation hydrique et thermique de matériaux de génie civil à faibles impacts environnementaux*, Thèse de Doctorat, INSA de Rennes, 2004.
- [10] V. Cerezo, *Propriétés mécaniques, thermiques et acoustiques d'un matériau à base de particules végétales: approche expérimentale et modélisation théorique*, Thèse de Doctorat, INSA & ENTPE de Lyon, 2005.
- [11] A. Evrard, *Transient hygrothermal behaviour of lime–hemp materials*, Thèse de doctorat de sciences de l'ingénieur, Ecole polytechnique de Louvain Institut d'Architecture, 2008.
- [12] E.F. Sowell, P. Haves, Efficient solution strategies for building energy system simulation, *Energy and Buildings* 33 (2001) 309–317.
- [13] M.J. Cunningham, The moisture performance of framed structures: a mathematical model, *Building and Environment* 23 (1988) 123–135.
- [14] J. Bear, Y. Bachmat, *Introduction to Modeling of Transport Phenomena in Porous Media*, Kluwer Academic Publishers, Dordrecht, Netherlands, 1990.
- [15] C.R. Pedersen, Prediction of moisture transfer in building constructions, *Building and Environment* 27 (3) (1992) 387–397.
- [16] M. Künel, *Simultaneous Heat and Moisture Transport in Building Components*, Fraunhofer Institute of building physics, 1995, Available from: http://www.wufi.de/index_e.html.
- [17] N. Mendes, F.C. Winkelmann, R. Lamberts, P.C. Philippi, Moisture effects on conduction loads, *Energy and Building* 35 (7) (2003) 631–644.
- [18] J.R. Philip, D.A. De Vries, Moisture movement in porous materials under temperature gradients, *Transaction of American Geophysical Union* 38 (2) (1957) 222–232.
- [19] N. Mendes, I. Ridley, R. Lamberts, P.C. Philippi, Budag K, UMIDUS: A PC program for the prediction of heat and moisture transfer in porous building elements, in: *Building Simulation'99 Conference*, Kyoto, Japan, 1999, pp. 1–7.
- [20] N. Mendes, P.C. Philippi, A method for predicting heat and moisture transfer through multilayer walls based on temperature and moisture content gradients, *International Journal of Heat and Mass Transfer* 48 (2005) 37–51.
- [21] A.D. Tran le, C. Maalouf, K.C. Mendonça, T.H. Mai, E. Wurtz, Study of moisture transfer in doubled-layered wall with imperfect thermal and hydraulic contact resistances, *Journal of Building Performance Simulation* 2 (2009) 251–266.
- [22] L. Mora, E. Wurtz, K.C. Mendonça, C. Inard, Effects of coupled heat and moisture transfers through walls upon indoor environment predictions, *International Journal of Ventilation* 3 (3) (2004) 227–234.
- [23] E. Wurtz, F. Haghghat, L. Mora, K.C. Mendonça, C. Maalouf, H. Zhao, P. Bourdoukan, An integrated zonal model to predict transient indoor humidity distribution, *ASHRAE Transactions* 112 (2) (2006) 175–186.
- [24] C. Maalouf, E. Wurtz, L. Mora, F. Allard, Effect of free cooling on the operation of a desiccant evaporative system, *International Journal of Ventilation* 7 (2) (2008) 125–138.
- [25] L. Kristin, International Energy Agency, Annex 41—Subtask 1, Common Exercise, vol. 3, 2006.
- [26] IEA, Collection of reports of common exercise 1: Case 0A & Case 0B, International Energy Agency, Annex 41—Subtask, vol. 1, 2005.

- [27] M. Qin, R. Belarbi, A. Aît-Mokhtar, F. Allard, Simulation of couple heat and moisture transfer in air-conditioned buildings, *Automation in Construction* 18 (2009) 624–631.
- [28] S. Merakeb, F. Dubois, C. Petit, Modeling of the sorption hysteresis for wood, *Wood Science and Technology* 43 (7–8) (2009) 575–589.
- [29] H.M. Küzel, A. Holm, Zirkelbach, A.N. Karagiozis, Simulation of indoor temperature and humidity conditions including hygrothermal interactions with the building envelope, *Solar Energy* 78 (2005) 554–561.
- [30] O.F. Osanyintola, P. Talukdar, C.J. Simonson, Effect of initial conditions, boundary conditions and thickness on the moisture buffering capacity of spruce plywood, *Energy and Buildings* 38 (10) (2006) 1283–1292.
- [31] WUFI, Wärme und Feuchte instationär consultable sur: http://www.wufi.de/index_e.html (section: Basics, Moisture Storage Function).
- [32] B. Dolton, Hannah C, Cellular concrete: Engineering and technological advancement for construction in cold climates, in: The 2006 annual general conference of the Canadian Society for Civil Engineering, Alberta, Canada, 2006.